Original scientific paper
https://doi.org/10.33180/InfMIDEM2025.205

Informacije MIDEM
Journal of Microelectronics,
Electronic Components and Materials
Vol. 55, No. 2(2025), 115 – 125

Dual Band Reflectarray for Transmitter/Receiver Ground Station Drone Tracking Applications

Viwin Singh Yobuamalan[1], Ramesh Subramaniam[2], Sweetline Shamini Sureshkumar[3], and Chitra Sivathanu[4]

[1,2]Department of Electronics and Communication Engineering, SRM Valliammai Engineering College, Chennai, Tamil Nadu, India.
[3]Department of Electronics and Communication Engineering, Sri Sai Ram Institute of Technology, Chennai, Tamil Nadu, India.
[4]Department of Electronics and Communication Engineering, Rajalakshmi Engineering College, Chennai, Tamil Nadu, India.

Abstract: A dual-band, single-layer reflect array offering high gain has been developed for dual-polarized drone tracking applications. The reflect array unit comprises two center-notched spiral structures aligned orthogonally and is separated by an independent notch-perfect rectangle element. Based on the reflect array unit design, a single layer 7 x 7 array, totally 49 elements for Horizontally Linearly Polarized (HLP) Ku-band transmission (12.4 – 14.8 GHz) and 49 elements for Vertically Linearly Polarized (VLP) X-band reception (10.7 – 12 GHz is designed with the phase changes of over 75°. This phase changes is obtained by adjusting the length of the notched spiral patch within the unit cell. Two distinct horn sources has been implemented to energize the orthogonal ports, supplying separate linear polarization for each frequency band. The efficiency is about 18.2 to 22% across different frequency bands, underscoring the array's suitability for Drone Tracking applications. From the performance measures, it is found that the proposed dual-band reflect array is more suitable for drone ground station tracking applications. Additionally, this proposed structure minimizes design complexity and meets specifications of a low profile antenna with a simple structure and reduced weight.

Keywords: Dual-band, Reflect array, orthogonally linear polarization, single reflecting layer, Low Profile

Dvopasovni odsevni niz za oddajnik/sprejemnik zemeljske postaje za sledenje dronov

Izvleček: Razvit je bil dvopasovni enoslojni odbojni niz z visokim ojačenjem za dvo-polarizirane aplikacije sledenja dronov. Enota odbojnega polja je sestavljena iz dveh spiralnih struktur s središčnim zarezovanjem, ki sta pravokotno poravnani, ločuje ju neodvisni pravokotni element s popolnim zarezovanjem. Na podlagi zasnove enote odbojnega polja je zasnovano enoslojno polje 7 x 7, ki ima 49 elementov za oddajanje v pasu Ku (12,4-14,8 GHz) in 49 elementov za sprejemanje v pasu X (10,7-12 GHz) z vertikalno linearno polarizacijo (VLP) s faznimi spremembami nad 75°. Te spremembe faze se dosežejo s prilagajanjem dolžine spiralne zaplate z zarezami v enoti celice. Za napajanje ortogonalnih vrat sta bila uporabljena dva različna rogova, ki zagotavljata ločeno linearno polarizacijo za vsak frekvenčni pas. Učinkovitost je približno 18,2 do 22 % v različnih frekvenčnih pasovih, kar poudarja primernost polja za aplikacije sledenja dronov. Iz meritev učinkovitosti je razvidno, da je predlagano dvopasovno odbojno polje primernejše za aplikacije sledenja zemeljskih postaj dronov. Poleg tega ta predlagana struktura zmanjšuje zapletenost zasnove in izpolnjuje specifikacije nizkoprofilne antene z enostavno strukturo in manjšo maso.

Ključne besede: Dvopasovno, odbojni niz, ortogonalno linearna polarizacija, en odbojni sloj, nizek profil

** Corresponding Author's e-mail: viwinsingh3@gmail.com*

How to cite:
V. S. Yobuamalan et al., "Dual Band Reflectarray for Transmitter/Receiver Ground Station Drone Tracking Applications", Inf. Midem-J. Microelectron. Electron. Compon. Mater., Vol. 55, No. 2(2025), pp. 115–125

1 Introduction

The transmit and receive (Tx/Rx) communication in Drone Tracking Applications has garnered significant interest due to its ability to double the spectrum efficiency. To achieve this, high transmit-receive (Tx/Rx) isolation at the antenna layer is required, which helps reduce the complexity and cost in wireless communication systems. Hence, several Tx/Rx antennas like co-polarized shared aperture scheme with high isolation have been developed. However, extending these co-polarized designs to large-scale arrays can be complex.

Reflect array antennas known for their high gain and simple feeding mechanisms have been formulated. It typically have narrow bandwidths, but modifying the f/D ratio and aperture size can increase it by about 10% [1-2]. To make the aperture smaller and reduce cross polarization, the elements of the RA are fine-tuned using a multilayered RAs. Although these are more constructive but leads to misalignment errors [3].

Multilayer reflect arrays can enhance bandwidth by over 15%, though they are challenging to design, expensive to fabricate, and heavier than single-layer structures. To allow system frequencies to share the same aperture in a single layer, they need to be widely separated [4]. Thus, Multi-resonant single-layer elements achieve phase variation at two distinct bands by varying patch length. Three interconnected dipoles in a single layer achieve various polarizations, but wide spacing may lead to impractically large inner element spacing and narrow element patterns [5]. A design of a wide band single layer reflect array antenna using a new broadband cell is proposed [6, 7]. Single-layer dual-band circularly polarized reflect arrays combine devices operating on different frequency bands, though with relatively high side-lobe levels and cross-polarization due to high-frequency components [8]. Designs like a single reflecting layer with curved double cross elements cater to dual-band linearly polarized operation. Dielectric layers with phase delay lines and circular patches with slots are used for X-band and K-band operation. Additionally, designs using square rings with slots and parallel dipoles in a single layer demonstrate phase shift and operation in two distinct frequency bands. Circular patches added to ring structures with a single dielectric layer offer dual-band capabilities. A dual-frequency reflect array with three layers of patches of differing sizes is described, although it incurs significant processing costs due to structural complexity [9-14]. However, multilayer reflect array antennas restrict transmission phase, diminishing overall performance. Profile reduction can be achieved by reducing the number of layers, resulting in low-profile structures with high radiation efficiency and simple designs [15-18].

Dual-band reflect arrays often use two layers, making them more complex and expensive to produce. They also become heavier, which is not ideal for many uses. Single-layer elements are better because they are cheaper, lighter and easier to make [19-23]. So, this work focused on single layer elements Dual Band Reflect Array for Tx/Rx Ground Station Drone Tracking Applications.

2 Antenna design

Thus, a formulated basic single-layer microstrip element is shown in Figure 1a.

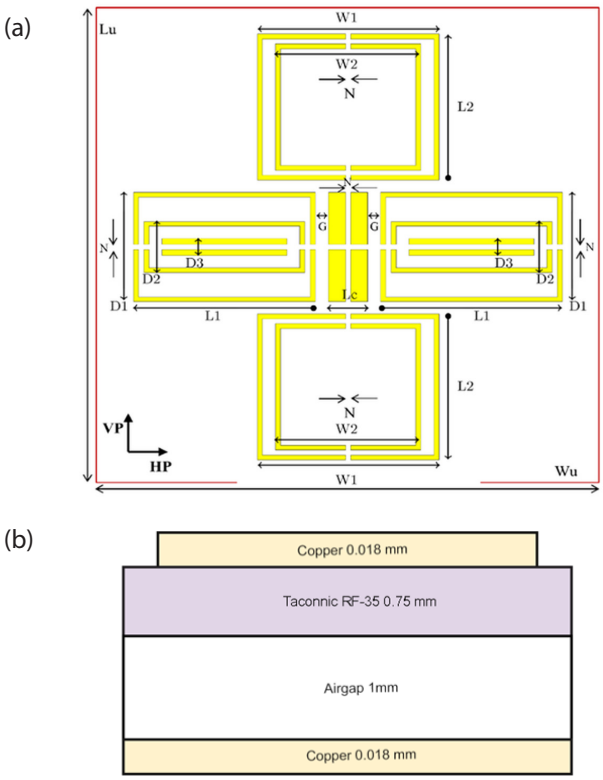

Figure 1: Geometry of unit cell in mm (a) top view b) side view

The radiating patches of the unit element module are in the shape of rectangular spirals. The rectangular spiral patches are evenly spaced relative to the origin and perpendicular to the axis of the unit cell. The horizontal centre notched spiral loop element is accountable for the horizontal linear polarized reflect array, while the vertical centre notched spiral loop element is accountable for the vertical linear polarized reflect array.

The notched rectangle element is positioned in the middle between the dual elements for polarization diversity between the operating bands and to decrease cross polarization. Horizontal and vertical elements

are positioned orthogonally and independently. This single-layer component eliminates a number of design flaws that were present in the previous designs [24-26]. In this design, there are no spatial restrictions on the elements, and they are all independent of one another.

By introducing a notch in the centre of a spiral structure, perfect orthogonal linear polarization at two frequencies can be supported. The reflect array structure is very simple and easy to fabricate, and it provides a high degree of polarization diversity. By varying the horizontal spiral loop length L1 achieved nearly 75° phase shift similarly the vertical spiral loop length L2 achieved nearly 78° phase shift. The dual element changing their length provides the smooth phase response independently.

2.1 Design and study of unit cell

The unit cells are etched on a standard Taconic RF 35 substrate, which has a dielectric constant of 3.55 and a thickness of 0.76 mm. The ground plane for transmitting and receiving frequencies is a conventional copper plane. The floquet port is used to model the unit cell structures, and a periodic boundary condition is established. A comprehensive wave analysis is then performed using the incident plane that is normal to the unit cell axis. The unit cell for transmitter frequencies is built for linear horizontal polarization. Similarly, the receiver is designed for linear vertical polarization. The unit cell performance is critical in determining the radiation performance of the planned array. To reduce phase errors, a phase range of 360 degrees or greater is required. Obtaining a smooth linear phase versus length response is also critical. The width L1 is changed to achieve a wide phase range for the transmit band's centre frequency. The width L2 is changed to obtain a large phase range for the receiver band's centre frequency [27].

2.1.1 Phase ranges for transmit band and receive band

The required phase shift at each element in flat reflect array unit cell is obtained from [1],

$$\varphi_R = K_0\left(d_i - \left(x_i cos\varphi_b + y_i\, sin\varphi_b\right) sin\,\theta_b\right) \qquad (1)$$

where, K_0 = propagation constant in vacuum, d_i = distance from phase center of the horn feed to the individual cell, (x_i, y_i) = the co-ordinates of element i. (φ_b, θ_b) = beam azimuth and elevation angle from the source.

Varying the length changes the impedance and therefore the refection phase-shift is changed. To verify this, the reflected phase versus length response for the center frequency is examined for polarization modes and is shown in figure 2a and 2b.

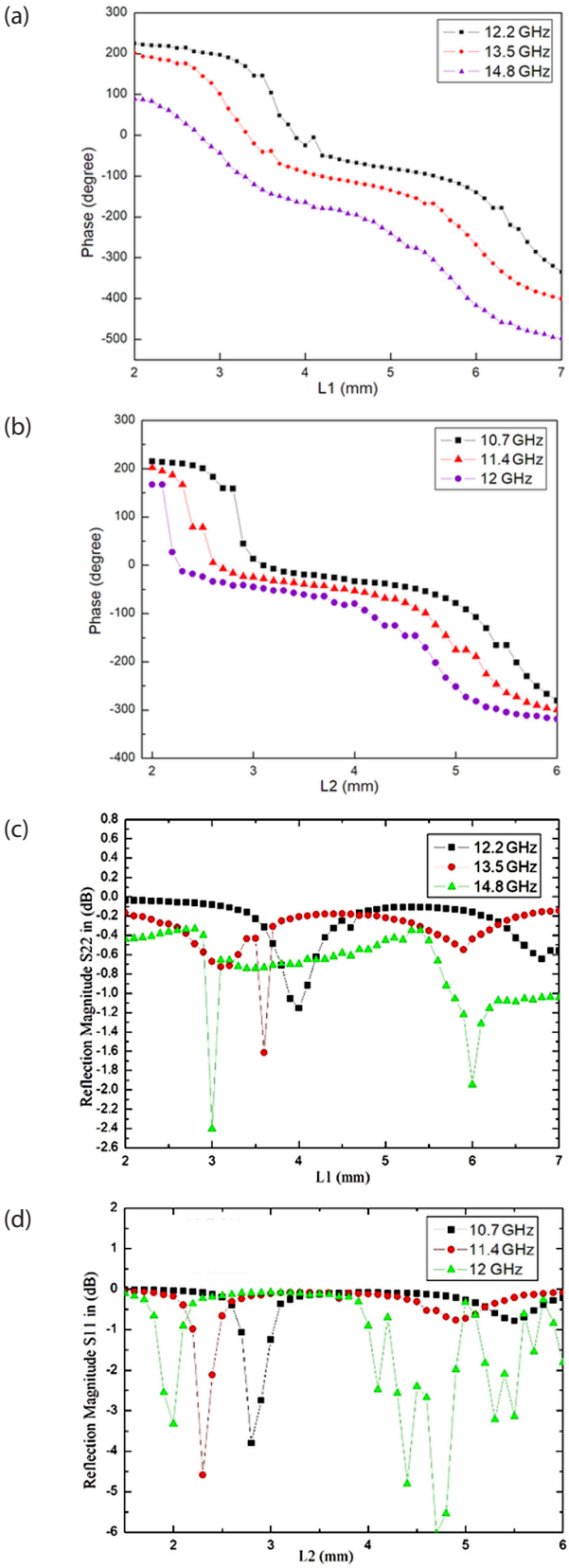

Figure 2: Reflection phase and magnitude of unit cell (a) Reflection Phase Ku-band. (b) Reflection Phase X-band. (c) Reflection magnitude Ku-band. (d) Reflection magnitude X-band.

Here, Ansoft HFSS simulation software, which provides master-slave boundaries and Floquet Ports to model repeating structures has been utilised. By changing the length, a phase shift and a change in the magnitude of the reflection field can be achieved, as shown in Figure 2.

A parametric sweep from 2 mm to 7 mm for L1 revealed a comprehensive reflected phase range exceeding 360 degrees for transmitter center frequencies, as shown in Figure 2(a) within CST MWS environment, configured for horizontal polarization (mode 2). However, in mode 1 (vertical polarization), the reflected phase range was limited to approximately 30 degrees (-140 to -170).

For reception frequencies, it's crucial that the reflecting element operates solely in linear vertical polarization, as confirmed by design findings. Remarkably, across all center frequencies in mode 1, an expansive phase range exceeding 360 degrees was observed, meeting vertical polarization requirements. Conversely, in mode 2, intentionally inferior performance was noted. Illustrated in Figure 2(B), the phase response for L2 values from 1 to 4 mm emphasizes the unit cell's exclusive operability in vertical polarization mode for receiver functionality, where it dominates in mode 1 and exhibits submissiveness in mode 2 within the complementary configuration.

The simulation results in Figures 2a and 2b show that the new unit cell has a wide linear phase range, about 500° and 300°, for the frequencies studied in the Ku and X bands. The graphs reveal that the phase response is similar at nearby frequencies. This feature can enhance the bandwidth in both frequency bands. So it can considered that all the elements are normally illuminated.

As shown in Figures 2a and 2b, when L increases, the reflection phase curve becomes more linear and the phase range also increases. Additionally, the reflection magnitude changes as the length varies.

Figure 3 shows the current distribution. Even though strong currents are generated on the resonator, the loss

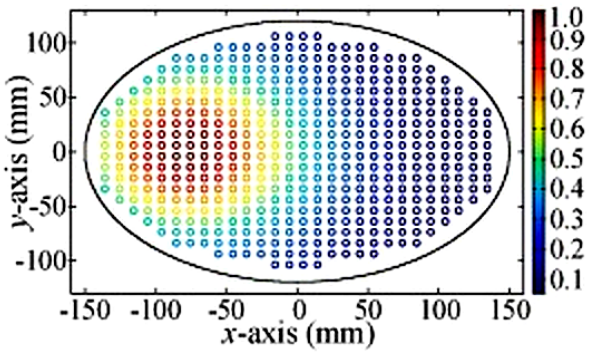

Figure 3: Current distribution

remains low because the copper has good conductivity and the substrate has almost no loss tangent. Since the loss is very small, it doesn't need to be considered in the design of the refractory antenna.

To improve scanning gain, this design keeps the positions of the feeding horns fixed. The Tx and Rx beams in the boresight direction are mainly set by the elements lined up with the feeding horns. Figure 4 shows the calculated radiation patterns based on the array factor and element pattern.

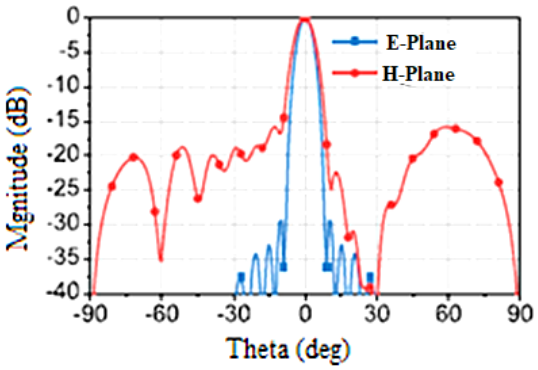

Figure 4: Radiation Patterns

The array can produce broadside radiations in both main planes. The E-plane has normal radiation, but the side lobes in the H-plane are quite strong. This indicates that the phase distribution of the other half of the array (along the positive x-axis) can impact the H-plane's radiation performance (side lobes). To reduce these side lobes, a phase distribution optimization scheme is introduced. Thus, the optimised design parameters of the proposed antenna is depicted in Table 1.

Table 1: Parameter value of the design

Parameter	Value (mm)
N	0.2
Lc	1.5
T	0.76
Tg	1
W1	7.5
W2	7
D1	7
D2	4.5
D3	1.25
Wu	19.3
Lu	19.3
G	1

Where,
N - Centered notch size (in both horizontal and vertical)
Lc -independent center notched rectangle element length,
T - Substrate thickness,

Tg -Air gap thickness,
W1 and W2 - vertical element width,
D1 and D2 - horizontal element width,
Wu and Lu - unit cell length and width.
L1 and L2 - varying horizontal and vertical spiral length for phase responses.

(a)

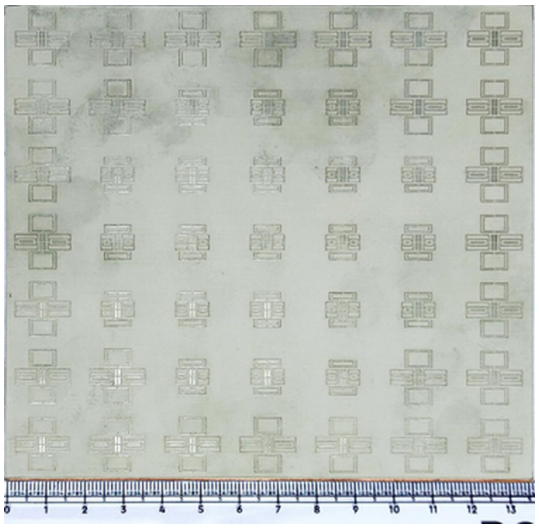

(b)

(c)

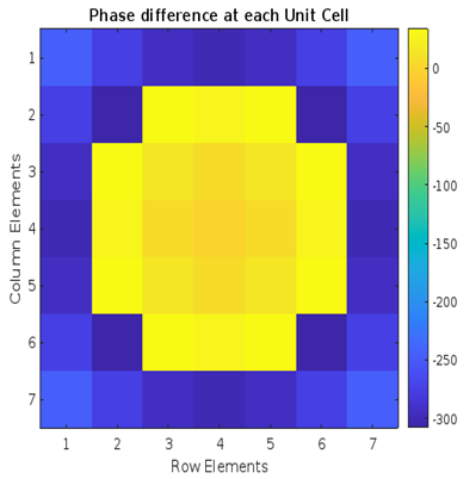

Figure 5: Fabricated single layer reflect-array antenna (a) Top View (b) Bottom view (c) Phase distribution diagram

3 Results and discussion

The unit cell elements were used to create a 7 × 7 array, resulting in a single layer that measures 135.66 mm by 135.66 mm. This array was made on a standard Taconic RF-35 lossy substrate, which has a dielectric constant of 3.55 and a thickness of 0.76 mm, with a loss tangent of 0.0018. The elements of the array were etched onto the substrate. There is a 1 mm thin air gap layer between the substrate and the ground plane to allow for wide bandwidth. The required phase for each individual element, based on its position, is listed in Table 2 is calculated using Equation (1).

The array is simulated with the CST MWS time domain solver, with the normalized impedance set to 50 ohms before simulation. Radiation properties including main lobe level, main lobe beam width, and side lobe levels were examined. Figure 5 shows the fabricated single layer reflect-array antenna.

Figure 6 shows the measurement setup. A 7×7 element reflect array was placed at a distance from the feed horn, following the ratio f/D = 1. The feed horn was connected to a standard WR34 coaxial to waveguide adapter. The reflect array was tilted at 20° with a spacer and all these components were accumulated in a dielectric frame.

The source center feed comprises a pyramidal horn antenna with an F/D ratio set to 0.8. A full wave analysis was conducted for all six frequencies. The array was modeled using a waveguide port.

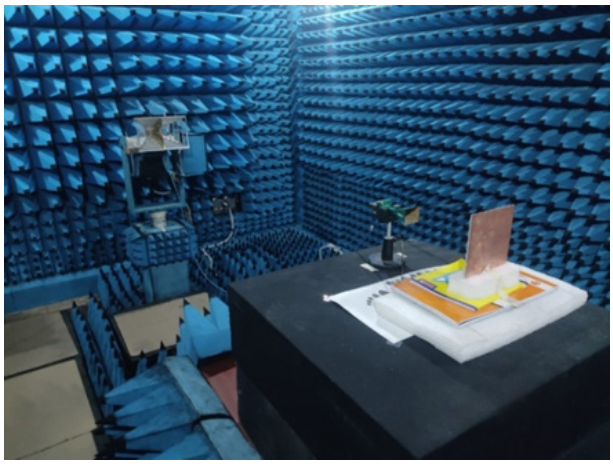

Figure 6: Measurement setup for the proposed reflect array antenna.

Figure 7 compares the measured and simulated gain radiation patterns. The measured and simulated patterns match well, although the measured gain is slightly lower than the simulated gain. These differences might be due to process errors and dielectric losses.

The results show that the fabrication process is effective. The transmission and reception efficiency of the reflect array antenna are 18% and 22%, respectively.

Figure 8 shows a comparison of the relative magnitudes of the simulated and measured patterns at different frequencies.

Figure 9 shows the measured S11 of the reflect array antenna. The S11 is below -14 dB in the frequency range from 10 GHz to 12.5 GHz.

These findings suggest that the developed prototype demonstrator exhibits good electrical performance and shows potential for applications in drone systems. For performance comparisons, Table 3 lists recently reported designs of single-layer dual-band antennas.

Table 3 shows a comparison of the fabricated reflect array with existing reflect array antennas. The results show that horn centre feed blockage reduces effi-

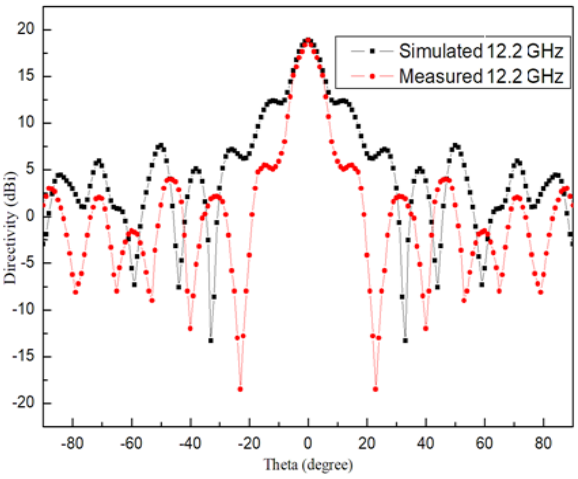

(a)

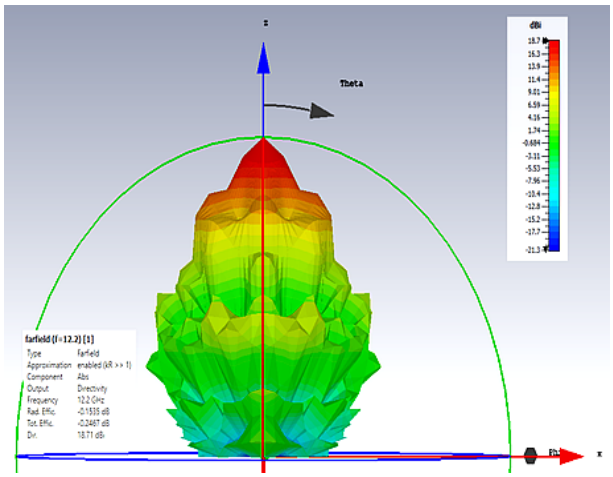

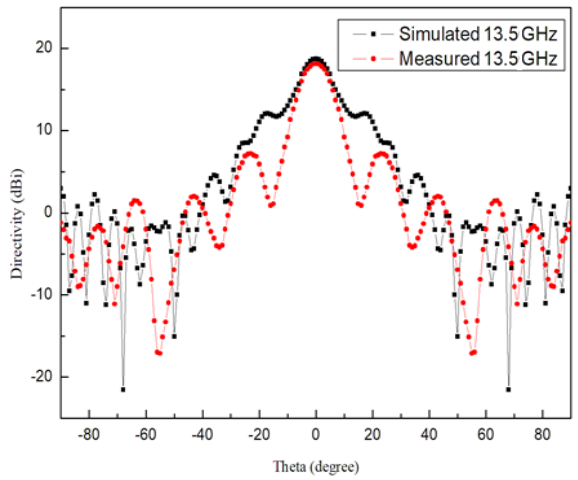

(b)

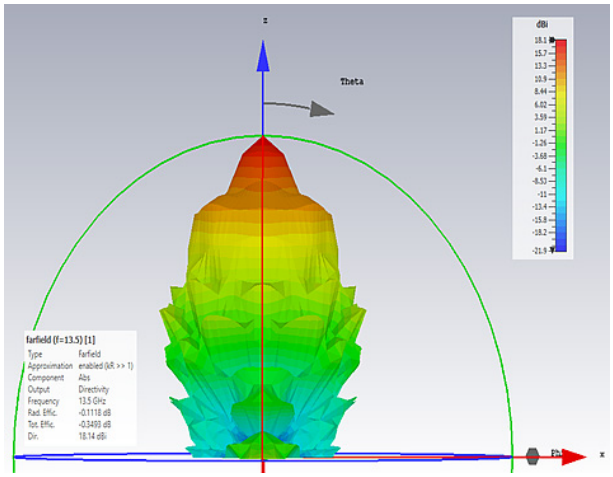

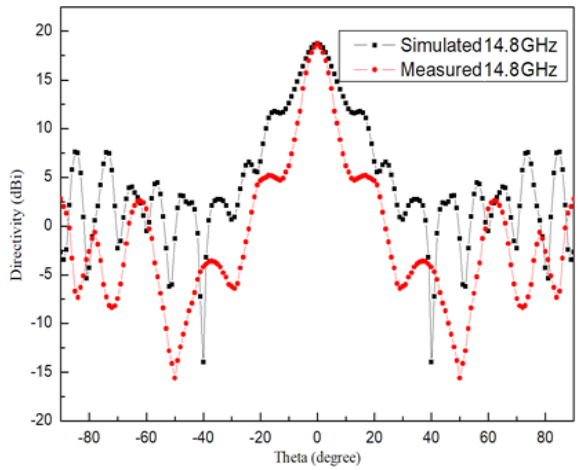

(c)

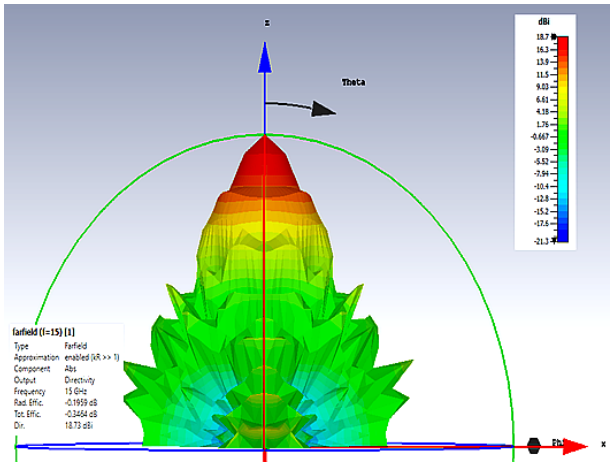

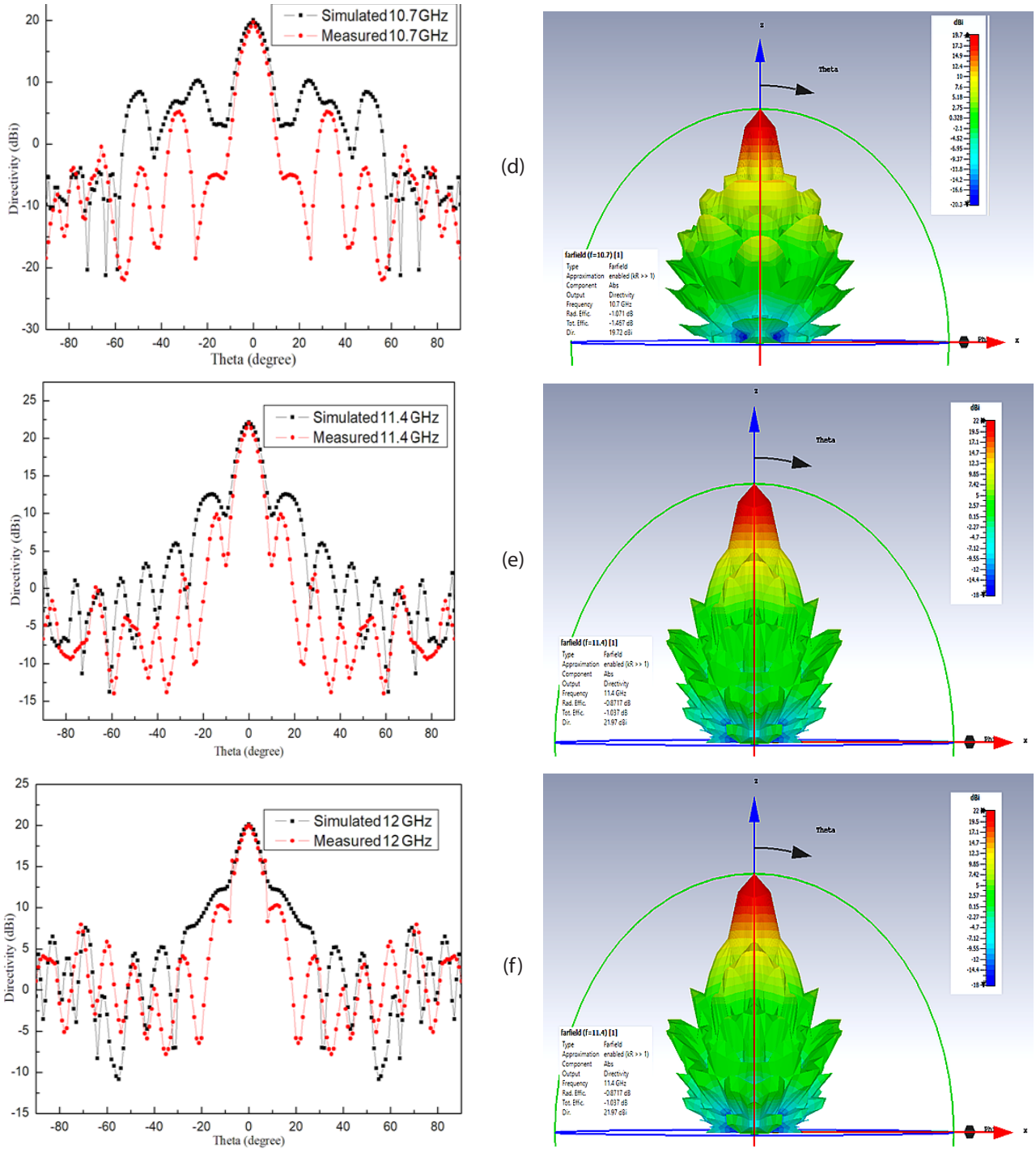

Figure 7: Simulated and tested reflect-array co-polarization radiation pattern comparison and 3D radiation pattern of transmitter bands (a) 12.2 GHz (b) 13.5 GHz (c) 14.8 GHz, receiver bands (d) 10.7 GHz (e) 11.4 GHz (f) 12 GHz

ciency. When the number of elements and aperture size of the tested reflect array antenna are compared, the higher gain is achieved. Furthermore, the ability to tune the phase of two bands independently simplifies dual band independent pattern isolation shaping at the transmitter and receiver.

4 Conclusion

This work developed a highly efficient 7 × 7 single-layer reflect array antenna with dual linear polarized modes designed for two distinct frequency bands. The incorporation of independent rectangular spirals for each band, along with strategically positioned notched square shapes within the unit cells, ensures effective

isolation between the dual elements. This proposed unit cell design presents a promising solution for various applications, including long-range communication for drone ground stations, tracker antennas, radar systems, and CubeSat satellite communication prototype unitcell, owing to its simplicity and compactness. This simulations have yielded impressive gains, with values ranging from 18.2 to 22 dBi across different frequency bands, underscoring the array's suitability for high-gain applications.

Table 2: Amount of phase shift (Degrees) required at each element position in 7 × 7 array and (L1/L2) normalized values (mm)

-146.6° (L1=5.95 mm / L2=4.47 mm)	157.32° (6 / 4.55)	122.6° (6.06 / 4.57)	110.83° (6.07 / 4.6)	122.6° (6.06 / 4.57)	157.32° (6 / 4.55)	-146.6° (5.95 / 4.47)
157.32° (6 / 4.55)	98.97° (6.15 / 4.58)	62.72° (3.62/ 2.54)	50.41° (3.65 / 2.55)	62.72° (3.62/ 2.54)	98.97° (6.15 / 4.58)	157.32° (6 / 4.55)
122.6° (6.06 / 4.57)	62.72° (3.62/ 2.54)	25.45° (3.67 / 2.58)	12.79° (3.68 / 2.6)	25.45° (3.67 / 2.58)	62.72° (3.62/ 2.54)	122.6° (6.06 / 4.57)
110.83° (6.07 / 4.6)	50.41° (3.65 / 2.55)	12.79° (3.68 / 2.6)	0° (3.7 / 2.62)	12.79° (3.68 / 2.6)	50.41° (3.65 / 2.55)	110.83° (6.07 / 4.6)
122.6° (6.06 / 4.57)	62.72° (3.62/ 2.54)	25.45° (3.67 / 2.58)	12.79° (3.68 / 2.6)	25.45° (3.67 / 2.58)	62.72° (3.62/ 2.54)	122.6° (6.06 / 4.57)
157.32° (6 / 4.55)	98.97° (6.15 / 4.58)	62.72° (3.62/ 2.54)	50.41° (3.65 / 2.55)	62.72° (3.62/ 2.54)	98.97° (6.15 / 4.58)	157.32° (6 / 4.55)
-146.6° (5.95 / 4.47)	157.32° (6 / 4.55)	122.6° (6.06 / 4.57)	110.83° (6.07 / 4.6)	122.6° (6.06 / 4.57)	157.32° (6 / 4.55)	-146.6° (5.95 / 4.47)

Table 3: Comparison of the tested reflect array with existing reflect array antenna

Ref.	Freq. (GHz)	No. of Substrate Layer	Elements Phase Range (degree)	Gain (dBi)	AE (%)	Polarization	Feed Type	Element Type
5	10/22	Single + Airgap	360 / 360	23/ 30	41/ 42	Dual LP	Center feed	Independent element with space limit
7	20/ 30	Single	More than 360	36/ 38	66.5/ 50	CP	Offset feed	Not an independent element
9	X/ K	Single + Airgap	400 / 500	26/ 29	47/25	Dual CP	Offset Feed	Not an independent with circular shape
10	X/ Ku	Single	530/ 780	23/ 25	46/33	CP	Center Feed	Independent elements with space limits. Outer border element gives space resistance.
11	X / Ku	Single	550 / 600	28 / 31	50 / 51	Dual LP	Center Feed	Independent elements. Dual elements varying length in both Horizontal and Vertical
12	X / K	Single + Airgap	400 / 400	27 / 31	63 / 42	Orthogonal LP	Center feed	Not an independent with circular shape
13	Ka / W	Dual	500/ 500	44 / 49	NA	LP	Offset feed	Independent elements situated in different layers
16	13.5 / 22	Three + Two Airgap	400 / 400	22 / 26	33 / 27	Dual LP	Center feed	Independent elements situated in different layers
Proposed work	10.7, 11.4, 12 / 12.2, 13.5, 14.8	Single + Air Gap	750 / 780	19.72, 22, 19.99 /18.87, 18.14, 18.73	47.8 / 21.3	Dual Orthogonal LP	Center Feed	Independent elements with band diversity. Not affect each other.

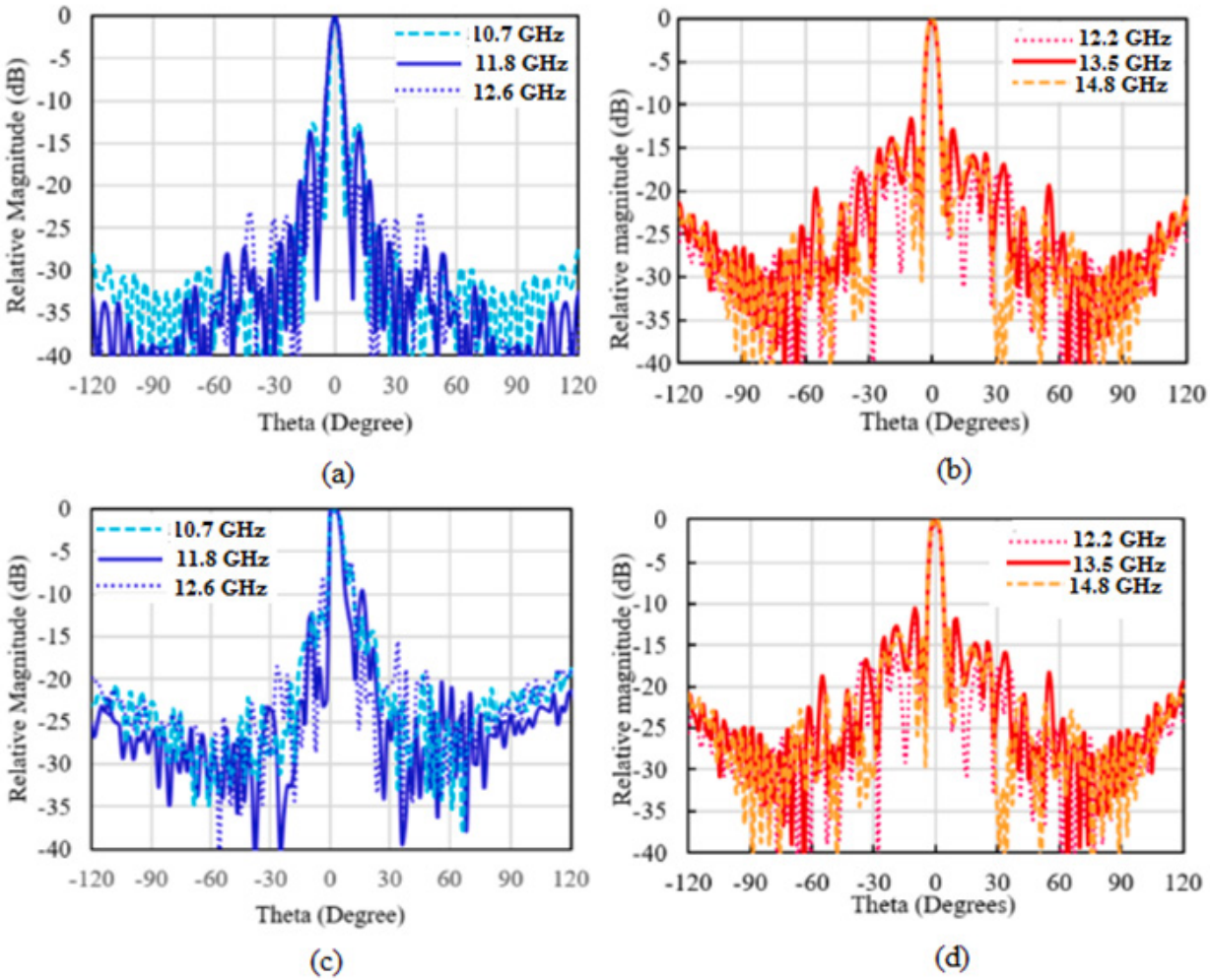

Figure 8: (a) Simulated H pattern at Receiver Band, (b) Simulated E pattern at Tx, (c) Measured H pattern at Rx, (d) Measured E pattern at Tx.

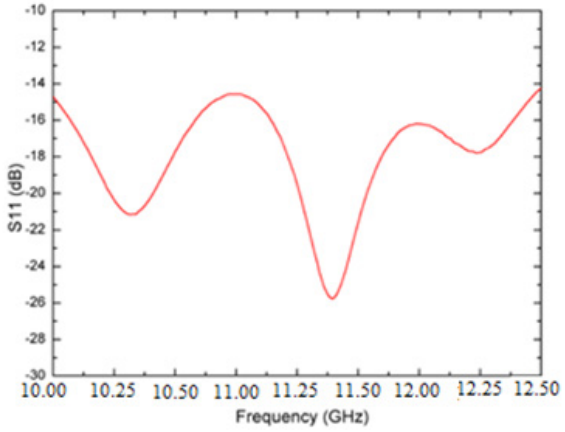

Figure 9: Measured S11 of the reflect array antenna

5 Conflicts of interest

The authors declare that they have no conflicts of interest to report regarding the present study.

6 Acknowledgment

The authors would like to thank DST-FIST for providing support facilities in the department of Electronics and Communication Engineering at SRM Valliammai Engineering College in Chennai, Tamil Nadu, India.

7 References

1. Imaz-Lueje, B., Prado, D.R., Arrebola, M. and Pino, M.R., 2020. Reflectarray antennas: A smart solution for new generation satellite mega-constellations in space communications. Scientific Reports, 10(1), p.21554. https://www.nature.com/articles/s41598-020-78501-0
2. Narayanasamy, K., Mohammed, G.N.A., Savarimuthu, K., Sivasamy, R. and Kanagasabai, M., 2020. A comprehensive analysis on the state-of-the-art developments in reflectarray, transmitarray, and

transmit-reflectarray antennas. International Journal of RF and Microwave Computer-Aided Engineering, 30(9), e22272. https://doi.org/10.1002/mmce.22272.
3. Prado, D.R., Arrebola, M., Pino, M.R. and Goussetis, G., 2020. Contoured-beam dual-band dual-linear polarized reflectarray design using a multiobjective multistage optimization. IEEE Transactions on antennas and propagation, 68(11), pp.7682-7687. https://doi.org/10.1109/tap.2020.2993014.
4. Han, C., Zhang, Y. and Yang, Q., 2017. Single-layer dual-band dual-linear-polarization reflectarray antenna with different beams for each band. Progress in Electromagnetics Research C, 73,65-73. https://doi.org/10.1109/tap.2016.2639023
5. Phua, Y.N., Lim, E.H. and Chung, B.K., 2020. Design of a single-layer broadband reflectarray using circular microstrip patch loaded with two unequal slots. AEU-International Journal of Electronics and Communications, 124, 153341. https://doi.org/10.1016/j.aeue.2020.153341.
6. Li, X. and Yang, L., 2020. Single-layer dual-band wide band-ratio reflectarray with orthogonal linear polarization. IEEE Access, 8, 93586-93593. https://doi.org/10.1109/ACCESS.2020.2986040.
7. Miklavčič, P. and Batagelj, B., 2024. A New Sum-Channel Radiating Element for a Patch-Monopole Monopulse Feed. Electronics, 13(16),p.3187. https://doi.org/10.3390/electronics13163187
8. Narayanasamy, K., Mohammed, G.N.A. and Arunkumar, S., 2024. A bandwidth-enhanced orthogonally polarized dual band reflectarray antenna. AEU-International Journal of Electronics and Communications, 176, 155155. https://doi.org/10.1016/j.aeue.2024.155155.
9. Elahi, M., Jeong, T., Yang, Y., Lee, K.Y. and Hwang, K.C., 2023. A wideband reflectarray antenna for satellite application with low cross-polarization. Applied Sciences, 13(7), p.4545. https://doi.org/10.3390/app13074545.
10. Ünaldı, S., Bodur, H., Cimen, S. and Çakır, G., 2020. RCS reduction of reflectarray using new variable size FSS method. AEU-International Journal of Electronics and Communications, 117, p.153098. https://doi.org/10.1016/j.aeue.2020.153098.
11. Tariq, S., Naseer, N., Iftikhar, A., Shafique, M.F., Nasir, J., Dahri, M.H., Fida, A. and Saka, B., 2023. Direct printable X-band low profile broadband reflectarray antenna using copper foils. AEU-International Journal of Electronics and Communications, 171, 154901. https://doi.org/10.1016/j.aeue.2023.154901.
12. Farooq, U., Iftikhar, A., Najam, A.I., Khan, S.A. and Shafique, M.F., 2023. An optically transparent dual-band frequency selective surface for polarization independent RF shielding. Optics Communications, 546, 129824. https://doi.org/10.1016/j.optcom.2023.129824.
13. Hashemi, S., Yahaghi, A. and Mohajeri, F., 2021. An optimization-based design of a wideband, polarization-independent reflectarray antenna at terahertz frequencies. Photonics and Nanostructures-Fundamentals and Applications, 45, p.100918. https://doi.org/10.1016/j.photonics.2021.100918.
14. Li, J., Mao, L. and Zhang, T., 2023. FSS sandwiched dual-frequency reflectarray for mobile communication applications. Electronics, 12(4), p.897. https://doi.org/10.3390/electronics12040897.
15. Song, W., Cai, Y., Xue, Q., Guo, N., Liu, K., Li, S., Wang, J. and Ding, H., 2022. X/Ku dual-band single-layer reflectarray antenna. Microwave and Optical Technology Letters, 64(9), pp.1621-1626. https://doi.org/10.1002/mop.33313.
16. qMalfajani, R.S. and Arand, B.A., 2017. Dual-band orthogonally polarized single-layer reflectarray antenna. IEEE Transactions on Antennas and Propagation, 65(11), pp.6145-6150. https://doi.org/10.1109/TAP.2017.2754459
17. Naseri P, Riel M, Demers Y, Hum SV. A dual-band dual-circularly polarized reflectarray for K/Ka-band space applications. IEEE Trans Antennas Propag. 2020; 68(6): 4627-4637. https://doi.org/10.1109/TAP.2020.2972650.
18. You, B.Q., Liu, Y.X., Zhou, J.H. and Chou, H.T., 2012. Numerical synthesis of dual-band reflectarray antenna for optimum near-field radiation. IEEE Antennas and Wireless Propagation Letters, 11, 760-762. https://doi.org/10.1109/LAWP.2012.2204229.
19. Dahri, M.H., Jamaluddin, M.H., Seman, F.C., Abbasi, M.I., Sallehuddin, N.F., I. Ashyap, A.Y. and Kamarudin, M.R., 2020. Aspects of efficiency enhancement in reflectarrays with analytical investigation and accurate measurement. Electronics, 9(11), p.1887. https://doi.org/10.3390/electronics9111887.
20. Encinar, J.A. and Zornoza, J.A., 2003. Broadband design of three-layer printed reflectarrays. IEEE Transactions on Antennas and Propagation, 51(7), pp.1662-1664. https://doi.org/0.1109/TAP.2003.813611
21. Ma, B., Lu, F., Zhi, G., Xue, X., Zhao, X., Ma, C., Fan, Y. and Yang, M., 2021. Development of an X-band reflectarray antenna for satellite communications. Scientific Reports, 11(1), p.6530. https://doi.org/10.1038/s41598-021-85132-6
22. Deng, R., Xu, S., Yang, F. and Li, M., 2017. Design of a low-cost single-layer X/Ku dual-band metal-only reflectarray antenna. IEEE Antennas and Wireless Propagation Letters, 16, pp.2106-2109. https://doi.org/10.1109/LAWP.2017.2698099

23. Yang, S., Yan, Z., Li, X. and Cai, M., 2022. Dual-band dual-polarized transmitarray with independent control of polarization at each band. International Journal of RF and Microwave Computer-Aided Engineering, 32(2), p.e22957. https://doi.org/10.1002/mmce.22957.
24. Abdelrahman, A.H., Elsherbeni, A.Z. and Yang, F., 2013. Transmission phase limit of multilayer frequency-selective surfaces for transmitarray designs. IEEE Transactions on Antennas and Propagation, 62(2), pp.690-697. https://doi.org/10.1109/TAP.2013.2289313
25. Raaza, A., Ramesh, S., Jerritta, S. and Rajendran, V., 2019. Circularly polarized circular slit planar antenna for vehicular satellite applications. The Applied Computational Electromagnetics Society Journal (ACES), pp.1340-1345. https://www.researchgate.net/publication/336319294_Circulary_Polarized_Circular_Slit_ Planar_Antenna_for_ Vehicular_Satellite_Applications
26. Abishek, E., Subramaniam, R., Ramanujam, P. and Esakkimuthu, M., 2023. Low-profile Circularly Polarized Conformal Antenna Array with Side Lobe Suppression for Vehicular SATCOM Applications. The Applied Computational Electromagnetics Society Journal (ACES), pp.439-447. https://doi.org/10.13052/2023.ACES.J.380608.
27. Hrovat, A., Kandus, G., Kuhar, U., Kelmendi, A. and Vilhar, A., 2016. A Ka-band satellite beacon receiver for propagation experiment. Informacije MIDEM, 46(1), pp.13-23.

Arrived: 27. 08. 2024
Accepted: 05. 03. 2025